FULL PAPER

Pharmacology

Cathepsin S degrades arresten and canstatin in infarcted area after myocardial infarction in rats

Akira SUGIYAMA[1)#], Ayaka MITSUI[1)#], Muneyoshi OKADA[1)*] and Hideyuki YAMAWAKI[1)]

[1)]Laboratory of Veterinary Pharmacology, School of Veterinary Medicine, Kitasato University, Higashi 23 bancho 35-1, Towada, Aomori 034-8628, Japan

ABSTRACT. The basement membrane surrounding cardiomyocytes is mainly composed of α1 and α2 chain of type IV collagen. Arresten and canstatin are fragments of non-collagenous C-terminal domain of α1 and α2 chain, respectively. We previously reported that the expression of canstatin was decreased in infarcted area 2 weeks after myocardial infarction in rats. In the present study, we investigated the regulatory mechanism for expression of arresten and canstatin. Myocardial infarction model rats were produced by ligating left anterior descending artery. Western blotting and immunohistochemical staining were performed to determine the protein expression and distribution. Arresten and canstatin were highly expressed in the heart. One day and three days after myocardial infarction, the expression of arresten and canstatin in infarcted area was lower than that in non-infarcted area. The expression of cathepsin S, which is known to degrade arresten and canstatin, was increased in the infarcted area. A knockdown of cathepsin S gene using small interference RNA suppressed the decline of arresten and canstatin in the infarcted area 3 days after myocardial infarction. This study for the first time revealed that arresten and canstatin are immediately degraded by cathepsin S in the infarcted area after myocardial infarction. These findings present a novel fundamental insight into the pathogenesis of myocardial infarction through the turnover of basement membrane-derived endogenous factors.

KEY WORDS: arresten, canstatin, cathepsin S, extracellular matrix, myocardial infarction

Myocardial infarction is the leading cause of cardiovascular death throughout the world [4, 16]. The ischemic stress (low oxygen and nutrition) induced by coronary artery occlusion during myocardial infarction leads to cardiomyocyte death, which causes cardiac dysfunction [30]. After myocardial infarction, compensated cardiac remodeling, such as scar formation in infarcted area and hypertrophy of remaining cardiomyocytes, occurs to make up for the decline of cardiac function [29, 31]. However, excessive cardiac remodeling induces pathological hypertrophy and fibrosis, which result in worsening of cardiac function. On the other hand, inadequate scar formation in infarcted area causes cardiac dysfunction and cardiac rupture [14]. Thus, an appropriate therapeutic strategy for cardiac remodeling after myocardial infarction has been awaited.

Extracellular matrix (ECM) proteins, such as collagen, fibronectin, laminin and proteoglycans, play a crucial role in tissue organization and regulate cellular functions of marginal cells [23, 32]. In the maintenance of tissue homeostasis, the balance between production and degradation of ECM proteins is properly kept. The ECM turnover is regulated by ECM degrading enzymes including matrix metalloproteinases (MMPs) and cathepsins [22, 32]. Abnormal ECM turnover is a key mediator for the development of pathological cardiac remodeling during cardiac diseases [8, 37]. Type IV collagen, a major component of basement membrane ECM, forms triple helical structure composed of α chains [7, 12]. The triple helix of two α1 and one α2 chains of type IV collagen called "classical chains" is expressed in whole body and is the main source of basement membrane surrounding cardiomyocytes [35, 36]. The non-collagenous C-terminal fragments of α chains of type IV collagen exert biological activities. For example, arresten and canstatin are potent anti-angiogenic factors derived from α1 and α2 chain, respectively [3, 10]. It has been reported that the expression of arresten is increased in the ischemia-reperfusion-injured myocardium in pigs [13]. We have demonstrated that canstatin is ubiquitously expressed in the normal heart tissue [28]. The biological function of arresten in the heart has not been investigated. On the other hand, we previously demonstrated that canstatin regulates functions of cardiac fibroblasts and myofibroblasts and exerts cardioprotective effects on H9c2 rat cardiomyoblasts [11, 18, 19, 28]. The biological

significance for arresten and canstatin in the normal heart remains to be elucidated.

We previously clarified that the expression of canstatin is decreased in the infarcted area 2 weeks after myocardial infarction in rats [28]. However, the regulatory mechanisms for expression of arresten and canstatin have not been fully clarified. In order to clarify them, we investigated the expression of arresten and canstatin in the infarcted area 1 day and 3 days after myocardial infarction in rats. Canstatin and arresten are known to be degraded by cathepsin S [33]. Thus, we also investigated whether a knockdown of cathepsin S gene affects the expression of arresten and canstatin after myocardial infarction.

MATERIALS AND METHODS

Reagents and antibodies

Reagents sources were as follows: Universal negative control small interference RNA (siRNA) and rat cathepsin S siRNA (Nippon Gene, Toyama, Japan). The target sequence of cathepsin S siRNA was as follows: sense 5′-GAAGCUUCCUAUCCCUACAdTdT-3′ and antisense 5′-UGUAGGGAUAGGAAGCUUCdTdT-3′.

Antibodies sources were as follows: Anti-arresten, anti-canstatin (Boster Biological Technology, Pleasanton, CA, U.S.A.), anti-cathepsin S, anti-vinculin (Santa Cruz Biotechnology, Santa Cruz, CA, U.S.A.), anti-total actin (Sigma-Aldrich, St. Louis, MO, U.S.A.), anti-rabbit IgG horseradish peroxidase linked whole antibody and anti-mouse IgG horseradish peroxidase linked whole antibody (Amersham Biosciences, Buckinghamshire, U.K. and Cell Signaling Technology, Beverly, MA, U.S.A.).

Animals

All animal studies were approved by the President of Kitasato University through the judgment by the Institutional Animal Care and Use Committee of Kitasato University (Approval No. 18-020, 17-083 and 16-033). Adult male Wistar rats (7–10-week old; CLEA Japan, Tokyo, Japan) were cared in accordance with the National Institutes of Health Guide for the Care and Use of Laboratory Animals and the Guideline for Animal Care and Treatment of the Kitasato University.

Isolation of organs from normal rats

After the rats were deeply anesthetized with an intraperitoneal injection with pentobarbital (100 mg/kg) or urethane (1.5 g/kg), kidney, left atrium, left ventricle, lung, subcutaneous adipose tissue, blood vessel (ventral aorta), skeletal muscle (hindlimb skeletal muscle), spleen, liver, stomach, colon, visceral adipose tissue (epididymal adipose tissue), testis and bladder were isolated. These organs were immediately frozen for protein extraction with liquid nitrogen and preserved at −80°C.

Myocardial infarction model rats

A permanent ligation of left anterior descending coronary artery was performed to make myocardial infarction model rats as described previously [27]. The rats were anesthetized with isoflurane [flow rate: 2 l/min, concentration: 5% (induction), 2.5% (maintenance)] through endotracheal tube connected to a vaporizer (respiratory rate: 100 times/min, tidal volume: 5 ml). A preoperative analgesia was achieved by a subcutaneous injection of buprenorphine (0.005 mg/100 g). Left thoracotomy between third or fourth intercostal space was performed, and the heart was exposed. Then the proximal left anterior descending artery was permanently ligated with a 6–0 nylon suture. After the chest was closed, rats were recovered and cared for 1 or 3 days. We confirmed the induction of myocardial infarction by a macroscopic observation of infarcted area and also by detecting the increase of apoptotic cells in infarcted area using a TdT-mediated dUTP nick end labeling (TUNEL) staining (n=3; data not shown).

In the experiments using siRNA, negative control siRNA or cathepsin S siRNA (10 μg) mixed with *in vivo*-jetPEI (Polypus transfection, Illkirch-Graffenstanden, France) (1.6 μl) at a nitrogen/phosphorus ratio of eight was diluted to 150 μl volume with 5% glucose. After the coronary ligation, these siRNAs were injected via right jugular vein as described previously [9].

Isolation of hearts from myocardial infarction model rats

One day and three days after the operation, the rats were deeply anesthetized with intraperitoneal injection of pentobarbital (100 mg/kg), and the hearts were isolated. The isolated hearts were washed with oxygenated Krebs-Henseleit solution (119 mM NaCl, 4.8 mM KCl, 2.5 mM CaCl$_2$, 1.2 mM KH$_2$PO$_4$, 1.2 mM MgSO$_4$, 24.9 mM NaHCO$_3$, 10.0 mM Glucose). For protein extraction, the hearts were separated into infarcted and non-infarcted area, which were immediately frozen with liquid nitrogen and preserved at −80°C. The remaining cross-sectional heart tissue was fixed with 10% neutral buffered formalin for immunohistochemical staining and TUNEL staining.

Western blotting

Western blotting was performed as described previously [27]. The isolated heart tissue was homogenized in frozen state with Cell destroyer (Bio Medical Science Inc., Tokyo, Japan), and total protein of the tissue was extracted by cell lysis buffer (Cell Signaling Technology). Equal amount of proteins (10 or 20 μg) was separated by sodium dodecyl sulfate-polyacrylamide gel electrophoresis (14%) and transferred to a nitrocellulose membrane. After blocked with 0.5% skim milk, the membranes were incubated with primary antibody against arresten (1:500 dilution), canstatin (1:500 dilution), cathepsin S (1:500 dilution), total actin (1:1,000 dilution), or vinculin (1:1,000 dilution) at 4°C overnight. The antibody against C-terminal domain of type IV collagen reacts with full-length type IV collagen [25]. Anti-arresten antibody recognizes both arresten (26 kDa: Figs. 1, 2, 5) and type IV collagen α1 (COL4A1; 190~200 kDa: Fig. 3). Anti-canstatin antibody recognizes both canstatin (24 kDa: Figs. 1, 2, 5) and
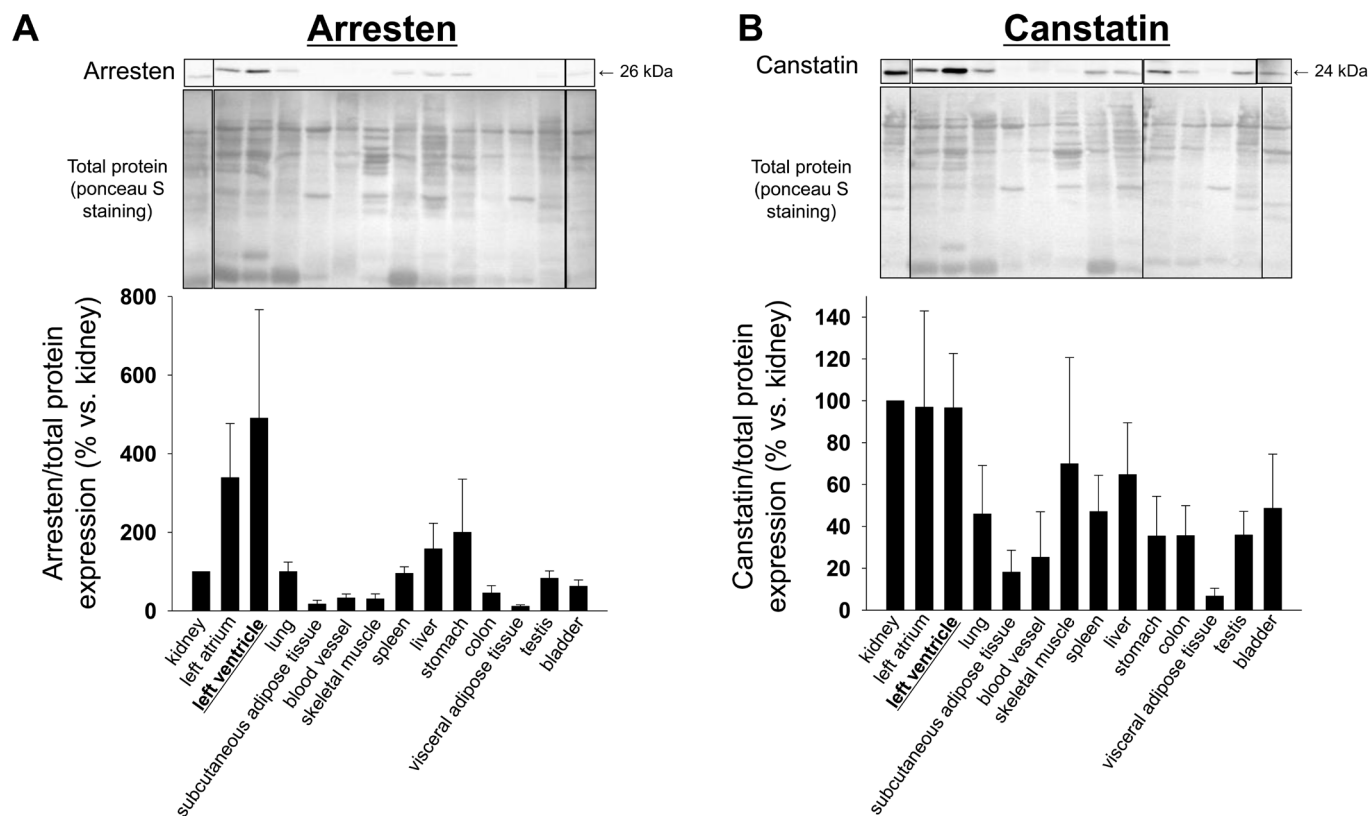
Fig. 1. Expression of arresten and canstatin in various organs of normal rats. The tissue proteins of male Wistar rats were extracted from various organs [kidney, left atrium, left ventricle, lung, subcutaneous adipose tissue, blood vessel (ventral aorta), skeletal muscle (hindlimb skeletal muscle), spleen, liver, stomach, colon, visceral adipose tissue (epididymal adipose tissue), testis and bladder]. The protein expression of arresten (A) and canstatin (B) was detected by Western blotting. (Upper) Representative blots for arresten (A: 26 kDa) and canstatin (B: 24 kDa) and total proteins stained with Ponceau S. were shown. (Lower) Levels of arresten (A) and canstatin (B) were corrected by total protein, and the normalized expression relative to kidney was shown as mean ± standard error of the mean (S.E.M.) (arresten: n=4; canstatin: n=5).

type IV collagen α2 (COL4A2; 185~195 kDa: Fig. 3). They were visualized using a horseradish peroxidase-conjugated secondary antibody and EZ-ECL detecting reagents (Biological Industries, Kibbutz Beit Haemek, Israel). The visualized protein expressions were detected using an ATTO light capture system (AE-6972; ATTO Co., Tokyo, Japan) and analyzed by using a CS Analyzer 3.0 software (ATTO Co.). The equal loading of proteins was examined by anti-total actin antibody or ponceau S staining (for a comparison among organs) (AppliChem, Darmstabt, Germany) as described previously [20]. The transferred membrane was incubated in a ponceau S staining solution (0.1% ponceau S in 5% acetic acid) at room temperature for 10 min. After washed by 1% acetic acid, the visualized band was analyzed by using CS Analyzer 3.0 software.

Immunohistochemical staining

Immunohistochemical staining was performed as described previously [27]. The cross-sectional heart tissue fixed with 10% neutral buffered formalin was embedded in paraffin, and thin sliced section (4 μm) of the heart tissue was made. After the deparaffinization, the sections were heated with microwave for activation of antigens in sodium citrate buffer (pH 6.0), and endogenous peroxidase activity was blocked by treating with 3% H_2O_2 for 10 min. Then, the sections were blocked with 5% normal goat serum and incubated with primary antibody against arresten (1:200 dilution), canstatin (1:200 dilution) or cathepsin S (1:50 dilution) at 4°C overnight. After washing, the sections were incubated in biotinylated link (Dako, Glostrup, Denmark) for 10 min and treated with streptavidin-horseradish peroxidase (Dako) for 10 min at room temperature. Then, expression of canstatin and arresten was visualized by a liquid 3,3′-Diaminobenzidine (DAB) + substrate chromogen system (Dako). The images were obtained using a light microscope (BX-51, OLYMPUS) equipped with a microscope digital camera (DP74, OLYMPUS). The positive area was quantified by using ImageJ software (National Institutes of Health, Bethesda, MD, U.S.A.).

TUNEL staining

TUNEL staining was performed by using Apoptosis *in situ* Detection Kit (Wako, Osaka, Japan) according to the manufacture's protocol. Briefly, the cross-sectional heart tissue fixed with 10% neutral buffered formalin was embedded in paraffin, and thin sliced section (4 μm) of the heart tissue was made. After the deparaffinization, the sections were reacted with protease solution for
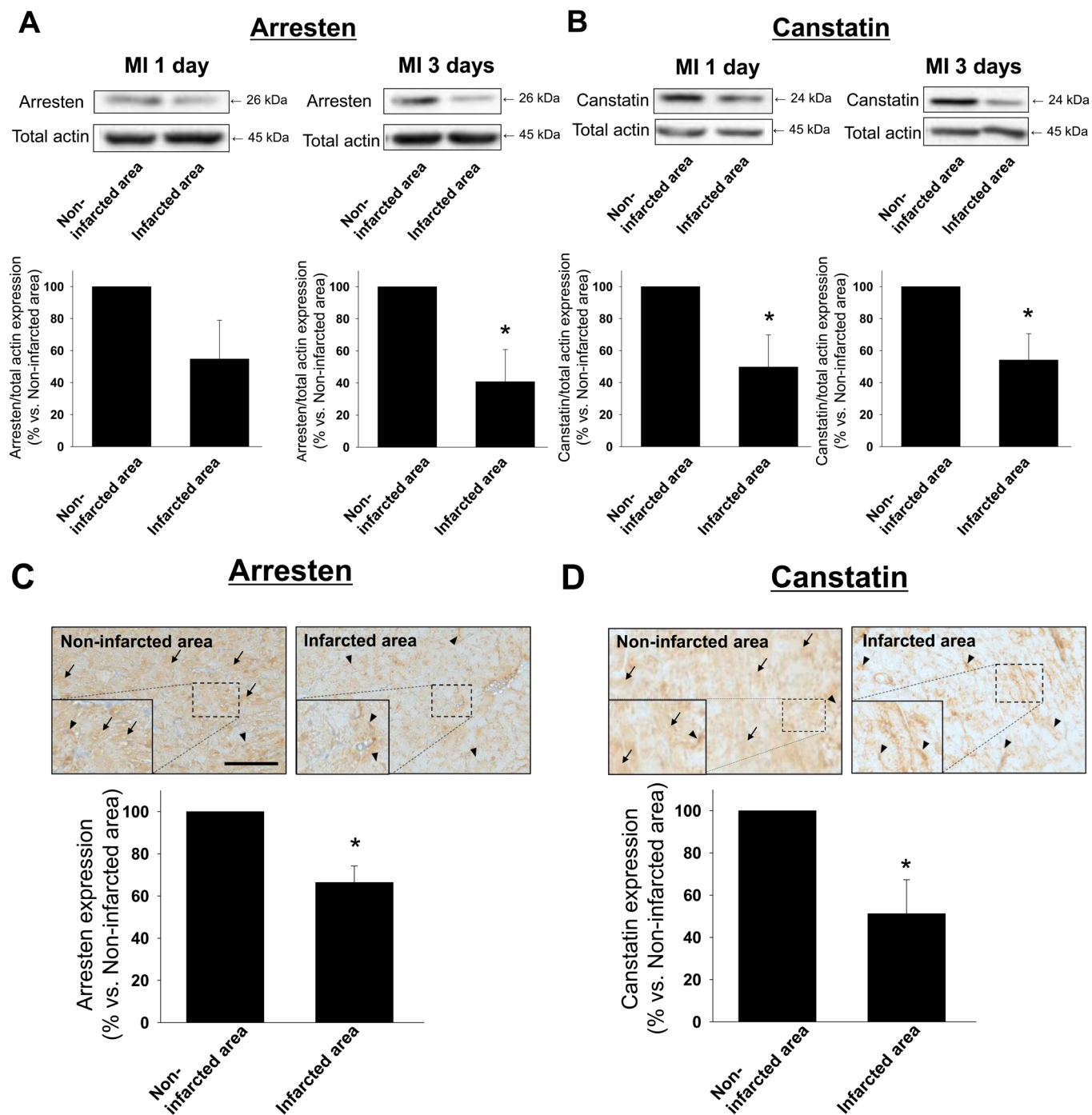
Fig. 2. Expression of arresten and canstatin in the infarcted area after myocardial infarction (MI). One day (A, B: left) and three days (A, B; right) after MI, the left ventricles were separated into non-infarcted and infarcted area, and the tissue proteins were extracted. Western blotting was performed to examine the expression of arresten (A) and canstatin (B). (A, B: Upper) Representative blots for arresten, canstatin and total actin (45 kDa) were shown. (A, B: Lower) Levels of arresten and canstatin were corrected by total actin, and the normalized expression relative to non-infarcted area was shown as mean ± S.E.M. (n=5). *$P<0.05$ vs. non-infarcted area. The cross sections of paraffin-embedded left ventricles from myocardial infarction (3 days) model rats were made. Immunohistochemical staining was performed by using anti-arresten (C) or anti-canstatin antibody (D). (C, D: Upper) Representative pictures were shown. Arrows show arresten- or canstatin-positive myocardium. Arrow heads show arresten- or canstatin-positive interstitial space. Scale bar: 100 μm. (C, D: Lower) The positive area (as shown in brown color) to anti-arresten or anti-canstatin antibody was calculated, and the normalized area relative to non-infarcted area was shown as mean ± S.E.M. (n=3). *$P<0.05$ vs. non-infarcted area.

5 min at 37°C, and then TdT reaction solution (TdT:TdT Substrate Solution=1:100) was applied for 10 min at 37°C. Endogenous peroxidase activity was blocked by 3% H_2O_2 for 5 min at room temperature. Then, the sections were incubated in peroxidase
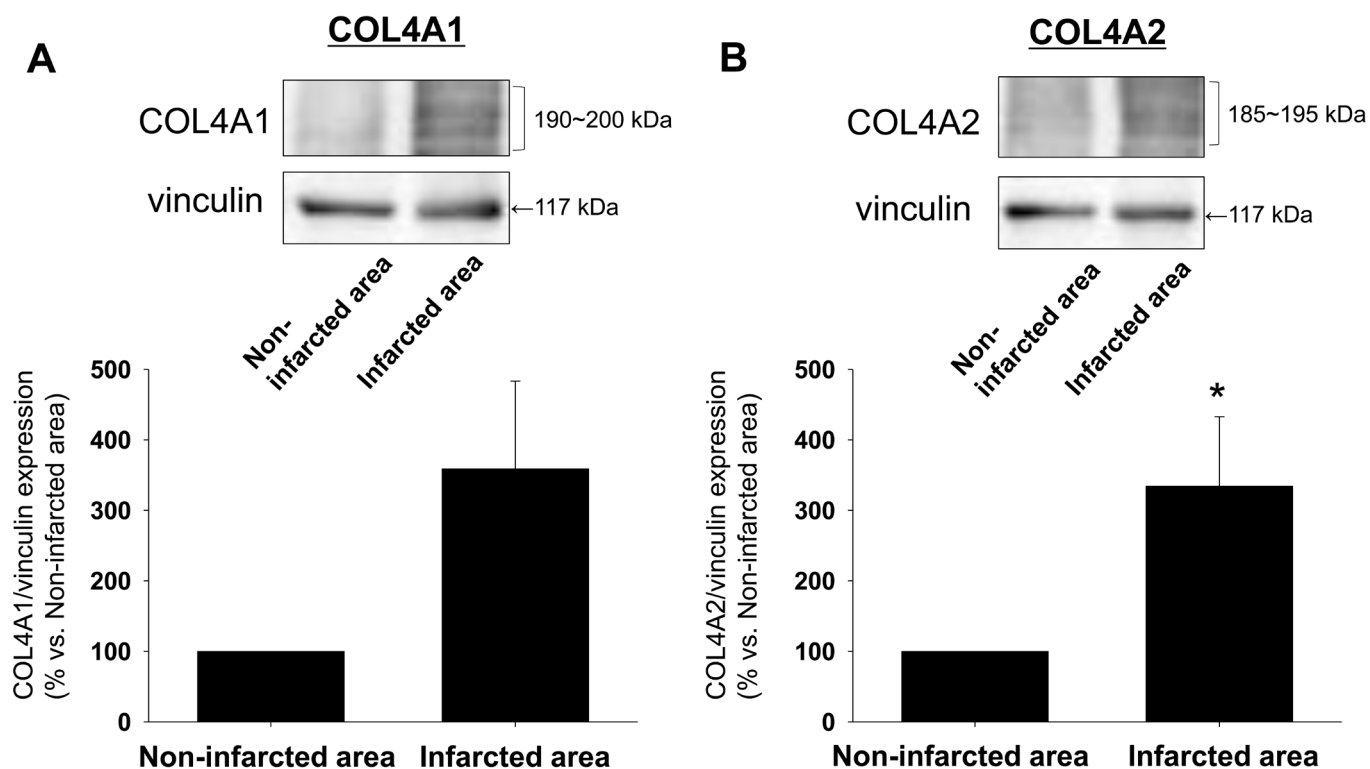
Fig. 3. Expression of type IV collagen α1 and α2 chain (COL4A1 and COL4A2) in the infarcted area after myocardial infarction. Three days after myocardial infarction, the left ventricles were separated into non-infarcted and infarcted area, and the tissue proteins were extracted. Western blotting was performed to examine the expression of COL4A1 (A) and COL4A2 (B). (Upper) Representative blots for COL4A1 (A: 190~200 kDa), COL4A2 (B: 185~195 kDa) and vinculin (117 kDa) were shown. (Lower) Levels of COL4A1 and COL4A2 were corrected by vinculin, and the normalized expression relative to non-infarcted area was shown as mean ± S.E.M. (n=5). *$P<0.05$ vs. non-infarcted area.

(POD)-conjugated antibody for 10 min at 37°C. Then, TUNEL positive nuclei were visualized by incubation with DAB + substrate chromogen system (Dako) for 5 min at room temperature. The nuclei were counterstained with hematoxylin. The images were obtained using a light microscope (BX-51) equipped with a microscope digital camera (DP74), and the TUNEL positive nuclei were counted in one high power field.

Statistical analysis

Data were shown as mean ± standard error of the mean (S.E.M.). Statistical evaluations were performed by Student's *t*-test. A value of $P<0.05$ was considered statistically significant.

RESULTS

Arresten and canstatin were highly expressed in the heart tissue of normal rats

We first examined the expression of arresten and canstatin in various organs. Both arresten and canstatin were widely expressed in many organs examined in this study (Fig. 1). Arresten was highly expressed in the heart tissue (left ventricle and left atrium) (n=4; Fig. 1A). Canstatin was also highly expressed in the heart tissue (left ventricle and left atrium) (n=5; Fig. 1B).

Expression of arresten and canstatin was decreased in the infarcted area

We examined the expression of arresten and canstatin in infarcted area 1 day and 3 days after myocardial infarction by Western blotting. The expression of arresten in infarcted area was decreased (at 1day, to 54.8 ± 24.1% vs. non-infarcted area; at 3 days, 40.8 ± 20.0%, $P<0.05$ vs. non-infarcted area) after myocardial infarction (n=5; Fig. 2A). The expression of canstatin in infarcted area was also decreased (at 1 day, to 49.7 ± 20.1%, $P<0.05$ vs. non-infarcted area; at 3 days, 54.1 ± 16.4%, $P<0.05$ vs. non-infarcted area) after myocardial infarction (n=5; Fig. 2B).

We next examined the distribution and expression of arresten and canstatin in infarcted area 3 days after myocardial infarction by using an immunohistochemical staining. Arresten and canstatin were widely expressed in both myocardium and interstitial space of non-infarcted area (n=3; Fig. 2C, 2D). In the infarcted area, the expression of arresten and canstatin in the myocardium was significantly decreased compared with non-infarcted area (arresten: 66.4 ± 7.8%, $P<0.05$ vs. non-infarcted area; canstatin: 51.2 ± 16.1%, $P<0.05$ vs. non-infarcted area) (n=3; Fig. 2C, 2D).
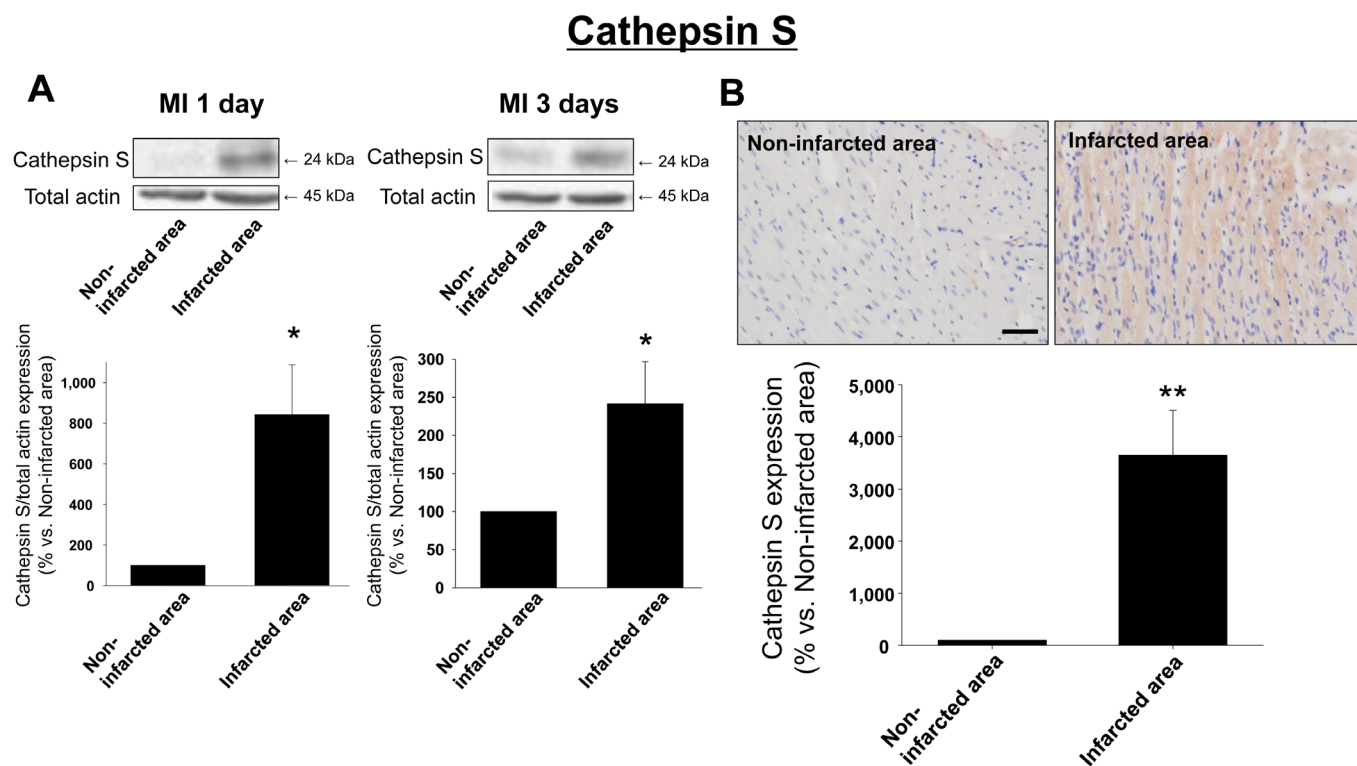
Cathepsin S

Fig. 4. Expression of cathepsin S in the infarcted area after myocardial infarction. (A) One day (left) and three days (right) after myocardial infarction, the left ventricles were separated into non-infarcted and infarcted area, and the tissue proteins were extracted. Western blotting was performed to examine the expression of cathepsin S. (Upper) Representative blots for cathepsin S (24 kDa) and total actin were shown. (Lower) Levels of cathepsin S were corrected by total actin, and the normalized expression relative to non-infarcted area was shown as mean ± S.E.M. (n=5). *$P<0.05$ vs. non-infarcted area. (B) The cross sections of paraffin-embedded left ventricles from myocardial infarction (1 day) model rats were made. Immunohistochemical staining was performed by using anti-cathepsin S antibody. The nuclei were counterstained with hematoxylin. (Upper) Representative pictures were shown. Scale bar: 50 μm. (Lower) The positive area to anti-cathepsin S antibody (as shown in brown color) was calculated, and the normalized area relative to non-infarcted area was shown as mean ± S.E.M. (n=4). **$P<0.01$ vs. non-infarcted area.

Expression of COL4A1 and COL4A2 was increased in the infarcted area

We also examined the expression of COL4A1 and COL4A2 in infarcted area 3 days after myocardial infarction by Western blotting. The expression of COL4A1 in infarcted area tended to be increased (358.8 ± 124.4% vs. non-infarcted area) compared with non-infarcted area (n=5; Fig. 3A). The expression of COL4A2 in infarcted area was significantly increased (334.3 ± 98.5%, $P<0.05$ vs. non-infarcted area) compared with non-infarcted area (n=5; Fig. 3B).

Cathepsin S expression was increased in the infarcted area, and its siRNA-injection suppressed the decline of arresten and canstatin expression

Cathepsin S is known to degrade arresten and canstatin *in vitro* [33]. The expression of cathepsin S in the infarcted area was significantly increased (at 1 day, to 842.3 ± 245.6%, $P<0.05$ vs. non-infarcted area; at 3 days, 241.7 ± 54.8%, $P<0.05$ vs. non-infarcted area) after myocardial infarction (n=5; Fig. 4A).

We next examined the distribution and expression of cathepsin S in infarcted area 1 day after myocardial infarction by using an immunohistochemical staining. Cathepsin S was hardly expressed in both myocardium and interstitial space of non-infarcted area (n=4; Fig. 4B). In the infarcted area, the expression of cathepsin S in the myocardium was significantly increased compared with non-infarcted area (3,653.5 ± 741.4%, $P<0.01$ vs. non-infarcted area) (n=4; Fig. 4B).

We performed an intrajugular injection of cathepsin S siRNA to clarify whether the induction of cathepsin S in infarcted area was responsible for the decrease of arresten and canstatin expression. We confirmed that the injection of cathepsin S siRNA suppressed the induction of cathepsin S protein in infarcted area 3 days after myocardial infarction (control siRNA: 323.1 ± 78.3% vs. non-infarcted area, $P<0.05$ vs. non-infarcted area; cathepsin S siRNA: 71.7 ± 16.8% vs. non-infarcted area) (control siRNA: n=4, cathepsin S siRNA: n=3; Fig. 5A). The knockdown of cathepsin S gene reversed the decrease of arresten (control siRNA: 32.0 ± 13.4%, $P<0.01$ vs. non-infarcted area; cathepsin S siRNA: 103.1 ± 29.4% vs. non-infarcted area) (control siRNA: n=4, cathepsin S siRNA: n=3; Fig. 5B) and canstatin (control siRNA: 50.5 ± 17.4%, $P<0.05$ vs. non-infarcted area; cathepsin S siRNA: 105.9 ± 47.4% vs. non-infarcted area) (control siRNA: n=4, cathepsin S siRNA: n=3; Fig. 5C) in infarcted area.
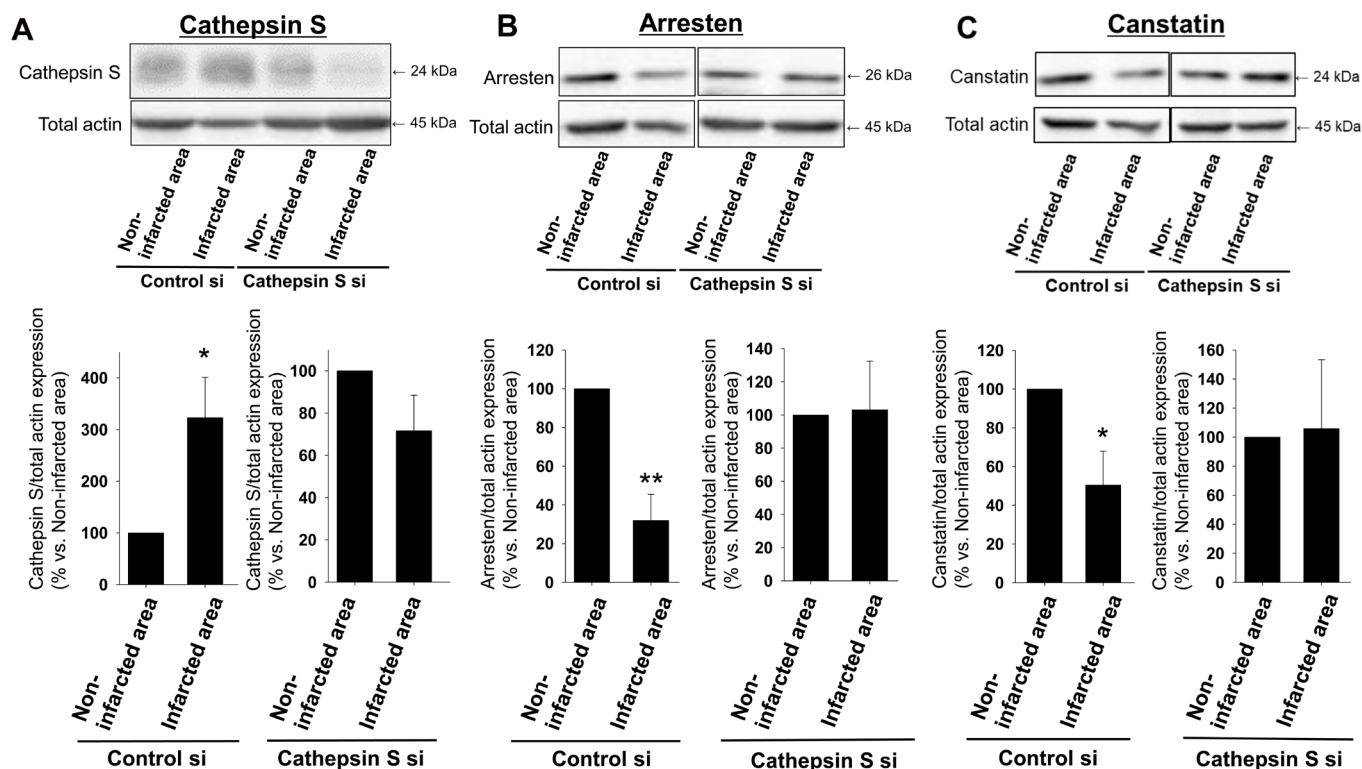
Fig. 5. Effects of cathepsin S gene knockdown on the expression of arresten and canstatin in infarcted area after myocardial infarction. An intra-jugular injection of cathepsin S small interference RNA (siRNA) or control siRNA with *in vivo* transfection reagent was performed immediately after myocardial infarction. Three days after myocardial infarction, the left ventricles were separated into non-infarcted and infarcted area, and the tissue proteins were extracted. Western blotting was performed to examine the expression of cathepsin S (A), arresten (B) and canstatin (C). (Upper) Representative blots for cathepsin S, arresten, canstatin and total actin were shown. (Lower) Levels of cathepsin S, arresten and canstatin were corrected by total actin, and the normalized expression relative to non-infarcted area was shown as mean ± S.E.M. (control siRNA: n=4, cathepsin S siRNA: n=3). *, **$P<0.05$, 0.01 vs. non-infarcted area.

Cathepsin S siRNA-injection had no effects on the pathology of myocardial infarction

We finally examined the effects of cathepsin S gene knockdown by siRNA-injection on apoptosis of cells in infarcted area by TUNEL staining. Cathepsin S siRNA had no effect on the number of apoptotic cells in infarcted area (n=3; Fig. 6).

DISCUSSION

This study for the first time demonstrated that the expression of arresten and canstatin is decreased perhaps through the degradation by cathepsin S in the infarcted area after myocardial infarction (Fig. 7).

In the present study, we revealed that various rat organs express arresten and canstatin. Type IV collagen α1 and α2 chains are known to be ubiquitously expressed in basement membrane of whole body including bronchus, blood vessel, alveolus, gland and glomerulus [5–7]. Thus, it is suggested that arresten and canstatin are widely expressed by degrading basement membrane composed of type IV collagen α1 and α2 chains. Among the organs examined, left atrium and ventricle highly expressed both arresten and canstatin (Fig. 1). The basement membrane surrounding cardiomyocytes is mainly composed of two α1 and one α2 chains of type IV collagen [35, 36]. ECM turnover, a production and degradation of ECM, is essential for the normal tissue homeostasis [26]. Thus, arresten and canstatin might be constantly released from the abundantly expressed type IV collagen in basement membrane of normal heart.

We previously demonstrated that the expression of canstatin was decreased in the infarcted area 2 weeks after myocardial infarction in rats [28]. In the present study, we demonstrated that the expression of arresten and canstatin was decreased even 1 day and 3 days after myocardial infarction in rats (Fig. 2). Thus, the reduction of arresten and canstatin might occur from an early stage of myocardial infarction. In contrast to our results, Lauten *et al.* reported that the expression of arresten was increased in ischemia-reperfusion model pigs under hypothermia [13]. However, the study did not determine the expression of 26 kDa arresten by Western blotting unlike this study. In the present study, we observed that arresten and canstatin were widely expressed in both myocardium and interstitial space of non-infarcted area. We previously showed that canstatin is expressed in normal cardiomyocytes [9]. In the present study, the reduction of arresten and canstatin was observed more often in myocardium after myocardial infarction (Fig. 2C, 2D). On the other hand, the expression of COL4A1 and COL4A2, a source for arresten and
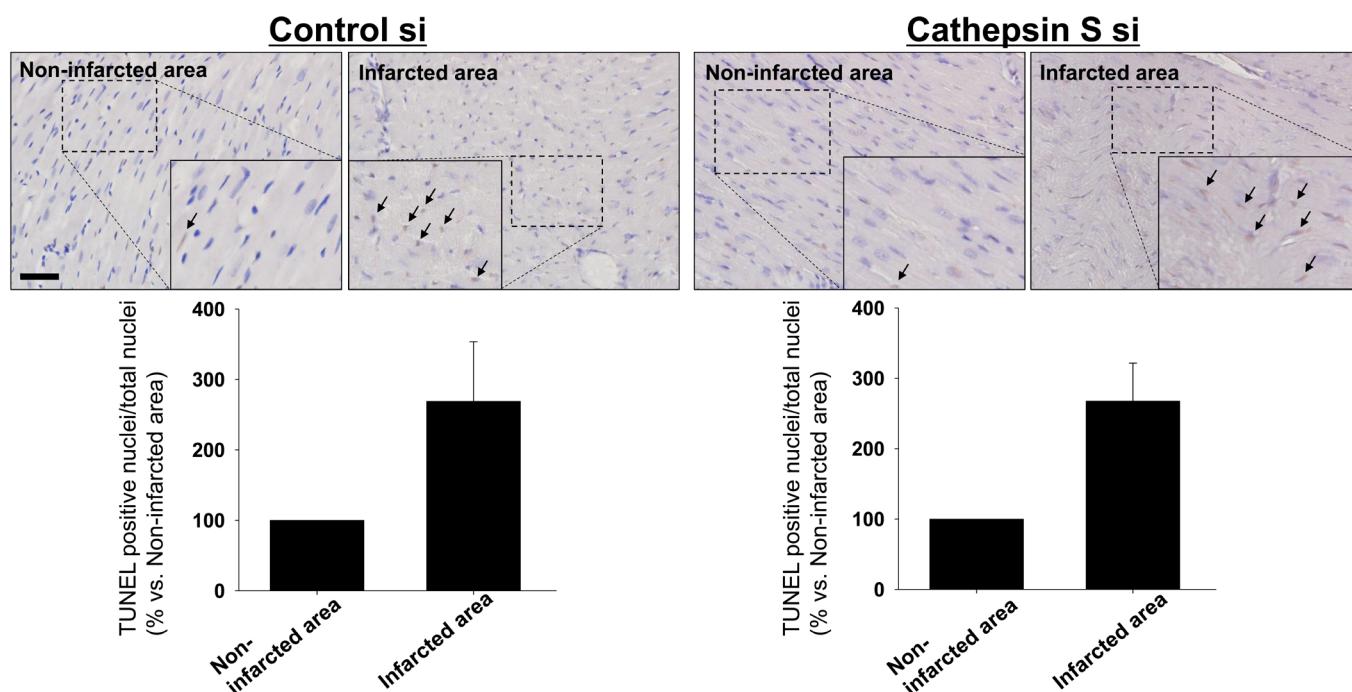
Fig. 6. Effects of cathepsin S gene knockdown on apoptosis of cardiomyocytes in infarcted area after myocardial infarction. The cross sections of paraffin-embedded left ventricles from cathepsin S siRNA- or control siRNA-injected myocardial infarction (3 day) model rats were made. TdT-mediated dUTP nick end labeling (TUNEL) staining was performed. The nuclei were counterstained with hematoxylin. (Upper) Representative pictures were shown. Arrows show TUNEL-positive nuclei (stained in brown color). Scale bar: 50 μm. (Lower) TUNEL-positive nuclei/total nuclei was calculated, and the normalized ratio relative to non-infarcted area was shown as mean ± S.E.M. (n=3).
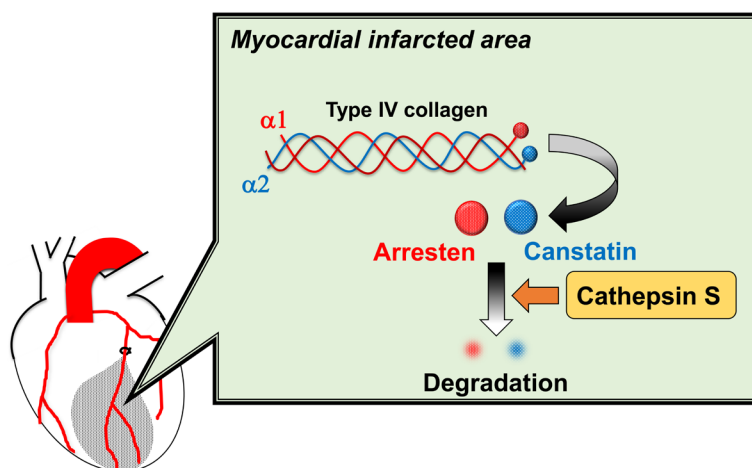

Fig. 7. Proposed model for the regulatory mechanisms of arresten and canstatin expression in myocardial infarcted area. The expression of arresten and canstatin derived from α1 and α2 chain of type IV collagen, respectively, is decreased perhaps through the degradation by cathepsin S in the infarcted area within a single day after myocardial infarction.

canstatin, was increased in the infarcted area after myocardial infarction (Fig. 3), which is consistent with the previous reports [15, 17, 36]. It has been reported that the increase in COL4A1 and COL4A2 expression was observed in interstitial spaces but not in myocardium [15, 17, 36]. Thus, it is suggested that arresten and canstatin are cleaved from interstitial type IV collagen and accumulated in cardiomyocytes, which might be degraded after myocardial infarction.

Cathepsin S, a cysteine protease localized in lysosomes, is expressed in various cardiovascular cells, such as cardiac fibroblasts, cardiomyocytes, vascular smooth muscle cells and endothelial cells [2]. *In vitro* study showed that cathepsin S degrades arresten and canstatin [33]. It has been reported that the expression and activation of cathepsin S are increased in the infarcted area of

myocardial infarction model mice [1]. This study revealed that the expression of cathepsin S was significantly increased in the infarcted area 1 day and 3 days after myocardial infarction (Fig. 4A). Cathepsin S is highly expressed in the cardiomyocytes of infarcted area (Fig. 4B). Thus, it is proposed that decline of arresten and canstatin expression in the infarcted area was caused by cathepsin S-dependent degradation in cardiomyocytes. Although cathepsin S was drastically increased in the infarcted area 1 day but not 3 days after myocardial infarction, the degree of decrease in the expression of arresten and canstatin did not differ between 1 day and 3 days. It is suggested that most of the constitutively expressed arresten and canstatin in cardiomyocytes are degraded rapidly 1 day after myocardial infarction by the highly expressed cathepsin S. On the other hand, the production from type IV collagen and degradation by cathepsin S for arresten and canstatin might be equilibrium in the infarcted area 3 days after myocardial infarction. The knockdown of cathepsin S gene by siRNA reverses the decrease of arresten and canstatin expression in infarcted area after myocardial infarction (Fig. 5). It is thus suggested that the increased cathepsin S might contribute to degrade arresten and canstatin in the infarcted area. Membrane type 1 (MT1)-MMP and MT2-MMP are proposed to be involved in the release of arresten and canstatin through the degradation of type IV collagen [21]. In the present study, we did not determine how arresten and canstatin are cleaved from type IV collagen after myocardial infarction. Further studies are needed to clarify the detailed regulatory mechanisms for production of arresten and canstatin.

The inhibition of cathepsin S induced apoptosis in tumor cells [24, 34, 38]. Chen *et al.* reported that cathepsin S exerted cardioprotective effects through the scar stabilization, since deficiency of cathepsin S or treatment with E64d, a non-selective cathepsin inhibitor, induced abnormal collagen turnover after myocardial infarction in mice [1]. On the other hand, E64d treatment had no effect on cardiomyocyte apoptosis in the border region adjacent to infarcted area [1]. We previously demonstrated that canstatin has a cytoprotective effect on hypoxia-induced apoptosis on H9c2 rat cardiomyoblasts [11]. Because the infarcted area suffers a hypoxic-stress, the decrease of canstatin in this area might cause cytotoxicity on cardiomyocytes. However, the inhibition of canstatin degradation by cathepsin S siRNA had no influence on cardiomyocyte apoptosis in infarcted area (Fig. 6). Cathepsin siRNA-injection had also no effect on fractional shortening, a parameter for cardiac function (control siRNA: n=4, cathepsin S siRNA: n=3; data not shown). Thus, the increase of cathepsin S and subsequent degradation of canstatin might not be involved in the cardiomyocyte apoptosis after myocardial infarction. It is a future issue to clarify the pathophysiological implication of the decrease of arresten and canstatin in the infarcted area after myocardial infarction.

In summary, we determined a part of the regulatory mechanisms of arresten and canstatin expression in the infarcted area after myocardial infarction. These results present a new fundamental insight into the pathogenesis of myocardial infarction through ECM turnover.

REFERENCES

1. Chen, H., Wang, J., Xiang, M. X., Lin, Y., He, A., Jin, C. N., Guan, J., Sukhova, G. K., Libby, P., Wang, J. A. and Shi, G. P. 2013. Cathepsin S-mediated fibroblast trans-differentiation contributes to left ventricular remodelling after myocardial infarction. *Cardiovasc. Res.* **100**: 84–94. [Medline] [CrossRef]
2. Cheng, X. W., Shi, G. P., Kuzuya, M., Sasaki, T., Okumura, K. and Murohara, T. 2012. Role for cysteine protease cathepsins in heart disease: focus on biology and mechanisms with clinical implication. *Circulation* **125**: 1551–1562. [Medline] [CrossRef]
3. Colorado, P. C., Torre, A., Kamphaus, G., Maeshima, Y., Hopfer, H., Takahashi, K., Volk, R., Zamborsky, E. D., Herman, S., Sarkar, P. K., Ericksen, M. B., Dhanabal, M., Simons, M., Post, M., Kufe, D. W., Weichselbaum, R. R., Sukhatme, V. P. and Kalluri, R. 2000. Anti-angiogenic cues from vascular basement membrane collagen. *Cancer Res.* **60**: 2520–2526. [Medline]
4. Finegold, J. A., Asaria, P. and Francis, D. P. 2013. Mortality from ischaemic heart disease by country, region, and age: statistics from World Health Organisation and United Nations. *Int. J. Cardiol.* **168**: 934–945. [Medline] [CrossRef]
5. Hasegawa, H., Naito, I., Nakano, K., Momota, R., Nishida, K., Taguchi, T., Sado, Y., Ninomiya, Y. and Ohtsuka, A. 2007. The distributions of type IV collagen α chains in basement membranes of human epidermis and skin appendages. *Arch. Histol. Cytol.* **70**: 255–265. [Medline] [CrossRef]
6. Hinenoya, N., Naito, I., Momota, R., Sado, Y., Kumagishi, K., Ninomiya, Y. and Ohtsuka, A. 2008. Type IV collagen alpha chains of the basement membrane in the rat bronchioalveolar transitional segment. *Arch. Histol. Cytol.* **71**: 185–194. [Medline] [CrossRef]
7. Hudson, B. G., Reeders, S. T. and Tryggvason, K. 1993. Type IV collagen: structure, gene organization, and role in human diseases. Molecular basis of Goodpasture and Alport syndromes and diffuse leiomyomatosis. *J. Biol. Chem.* **268**: 26033–26036. [Medline]
8. Hutchinson, K. R., Stewart, J. A. Jr. and Lucchesi, P. A. 2010. Extracellular matrix remodeling during the progression of volume overload-induced heart failure. *J. Mol. Cell. Cardiol.* **48**: 564–569. [Medline] [CrossRef]
9. Imoto, K., Hirakawa, M., Okada, M. and Yamawaki, H. 2018. Canstatin modulates L-type calcium channel activity in rat ventricular cardiomyocytes. *Biochem. Biophys. Res. Commun.* **499**: 954–959. [Medline] [CrossRef]
10. Kamphaus, G. D., Colorado, P. C., Panka, D. J., Hopfer, H., Ramchandran, R., Torre, A., Maeshima, Y., Mier, J. W., Sukhatme, V. P. and Kalluri, R. 2000. Canstatin, a novel matrix-derived inhibitor of angiogenesis and tumor growth. *J. Biol. Chem.* **275**: 1209–1215. [Medline] [CrossRef]
11. Kanazawa, H., Imoto, K., Okada, M. and Yamawaki, H. 2017. Canstatin inhibits hypoxia-induced apoptosis through activation of integrin/focal adhesion kinase/Akt signaling pathway in H9c2 cardiomyoblasts. *PLoS One* **12**: e0173051. [Medline] [CrossRef]
12. Kühn, K. 1995. Basement membrane (type IV) collagen. *Matrix Biol.* **14**: 439–445. [Medline] [CrossRef]
13. Lauten, A., Gerhard-Garcia, A., Suhr, F., Fischer, J. H., Figulla, H. R. and Bloch, W. 2014. Impact of ischemia-reperfusion on extracellular matrix processing and structure of the basement membrane of the heart. *PLoS One* **9**: e92833. [Medline] [CrossRef]
14. Ma, Y., de Castro Brás, L. E., Toba, H., Iyer, R. P., Hall, M. E., Winniford, M. D., Lange, R. A., Tyagi, S. C. and Lindsey, M. L. 2014. Myofibroblasts and the extracellular matrix network in post-myocardial infarction cardiac remodeling. *Pflugers Arch.* **466**: 1113–1127. [Medline]

15. Morishita, N., Kusachi, S., Yamasaki, S., Kondo, J. and Tsuji, T. 1996. Sequential changes in laminin and type IV collagen in the infarct zone-- immunohistochemical study in rat myocardial infarction. *Jpn. Circ. J.* **60**: 108–114. [Medline] [CrossRef]

16. Mozaffarian, D., Benjamin, E. J., Go, A. S., Arnett, D. K., Blaha, M. J., Cushman, M., Das, S. R., de Ferranti, S., Després, J. P., Fullerton, H. J., Howard, V. J., Huffman, M. D., Isasi, C. R., Jiménez, M. C., Judd, S. E., Kissela, B. M., Lichtman, J. H., Lisabeth, L. D., Liu, S., Mackey, R. H., Magid, D. J., McGuire, D. K., Mohler, E. R. 3rd., Moy, C. S., Muntner, P., Mussolino, M. E., Nasir, K., Neumar, R. W., Nichol, G., Palaniappan, L., Pandey, D. K., Reeves, M. J., Rodriguez, C. J., Rosamond, W., Sorlie, P. D., Stein, J., Towfighi, A., Turan, T. N., Virani, S. S., Woo, D., Yeh, R. W., Turner M. B., Writing Group Members American Heart Association Statistics Committee Stroke Statistics Subcommittee 2016. Heart disease and stroke statistics-2016 update a report from the American Heart Association. *Circulation* **133**: e38–e360. [Medline]

17. Murakami, M., Kusachi, S., Nakahama, M., Naito, I., Murakami, T., Doi, M., Kondo, J., Higashi, T., Ninomiya, Y. and Tsuji, T. 1998. Expression of the alpha 1 and alpha 2 chains of type IV collagen in the infarct zone of rat myocardial infarction. *J. Mol. Cell. Cardiol.* **30**: 1191–1202. [Medline] [CrossRef]

18. Okada, M., Morioka, S., Kanazawa, H. and Yamawaki, H. 2016. Canstatin inhibits isoproterenol-induced apoptosis through preserving mitochondrial morphology in differentiated H9c2 cardiomyoblasts. *Apoptosis* **21**: 887–895. [Medline] [CrossRef]

19. Okada, M., Murata, N. and Yamawaki, H. 2017. Canstatin stimulates migration of rat cardiac fibroblasts via secretion of matrix metalloproteinase-2. *Am. J. Physiol. Cell Physiol.* **312**: C199–C208. [Medline] [CrossRef]

20. Otani, K., Okada, M. and Yamawaki, H. 2017. Diverse distribution of tyrosine receptor kinase B isoforms in rat multiple tissues. *J. Vet. Med. Sci.* **79**: 1516–1523. [Medline] [CrossRef]

21. Rebustini, I. T., Myers, C., Lassiter, K. S., Surmak, A., Szabova, L., Holmbeck, K., Pedchenko, V., Hudson, B. G. and Hoffman, M. P. 2009. MT2-MMP-dependent release of collagen IV NC1 domains regulates submandibular gland branching morphogenesis. *Dev. Cell* **17**: 482–493. [Medline] [CrossRef]

22. Riaz, S., Zeidan, A. and Mraiche, F. 2017. Myocardial proteases and cardiac remodeling. *J. Cell. Physiol.* **232**: 3244–3250. [Medline] [CrossRef]

23. Rienks, M., Papageorgiou, A. P., Frangogiannis, N. G. and Heymans, S. 2014. Myocardial extracellular matrix: an ever-changing and diverse entity. *Circ. Res.* **114**: 872–888. [Medline] [CrossRef]

24. Seo, B. R., Min, K. J., Woo, S. M., Choe, M., Choi, K. S., Lee, Y. K., Yoon, G. and Kwon, T. K. 2017. Inhibition of cathepsin S induces mitochondrial ROS that sensitizes TRAIL-mediated apoptosis through p53-mediated downregulation of Bcl-2 and c-FLIP. *Antioxid. Redox Signal.* **27**: 215–233. [Medline] [CrossRef]

25. Shimizu, H., Aufschnaiter, R., Li, L., Sarras, M. P. Jr., Borza, D. B., Abrahamson, D. R., Sado, Y. and Zhang, X. 2008. The extracellular matrix of hydra is a porous sheet and contains type IV collagen. *Zoology (Jena)* **111**: 410–418. [Medline] [CrossRef]

26. Sonbol, H. S. 2018. Extracellular Matrix Remodeling in Human Disease. *J Microsc Ultrastruct* **6**: 123–128. [Medline] [CrossRef]

27. Sugiyama, A., Hirano, Y., Okada, M. and Yamawaki, H. 2018. Endostatin stimulates proliferation and migration of myofibroblasts isolated from myocardial infarction model rats. *Int. J. Mol. Sci.* **19**: E741. [Medline] [CrossRef]

28. Sugiyama, A., Okada, M. and Yamawaki, H. 2017. Pathophysiological roles of canstatin on myofibroblasts after myocardial infarction in rats. *Eur. J. Pharmacol.* **807**: 32–43. [Medline] [CrossRef]

29. Sutton, M. G. and Sharpe, N. 2000. Left ventricular remodeling after myocardial infarction: pathophysiology and therapy. *Circulation* **101**: 2981–2988. [Medline] [CrossRef]

30. Tavernarakis, N. 2007. Cardiomyocyte necrosis: alternative mechanisms, effective interventions. *Biochim. Biophys. Acta* **1773**: 480–482. [Medline] [CrossRef]

31. Turner, N. A. and Porter, K. E. 2013. Function and fate of myofibroblasts after myocardial infarction. *Fibrogenesis Tissue Repair* **6**: 5. [Medline] [CrossRef]

32. Valiente-Alandi, I., Schafer, A. E. and Blaxall, B. C. 2016. Extracellular matrix-mediated cellular communication in the heart. *J. Mol. Cell. Cardiol.* **91**: 228–237. [Medline] [CrossRef]

33. Wang, B., Sun, J., Kitamoto, S., Yang, M., Grubb, A., Chapman, H. A., Kalluri, R. and Shi, G. P. 2006. Cathepsin S controls angiogenesis and tumor growth via matrix-derived angiogenic factors. *J. Biol. Chem.* **281**: 6020–6029. [Medline] [CrossRef]

34. Wang, X., Xiong, L., Yu, G., Li, D., Peng, T., Luo, D. and Xu, J. 2015. Cathepsin S silencing induces apoptosis of human hepatocellular carcinoma cells. *Am. J. Transl. Res.* **7**: 100–110. [Medline]

35. Watanabe, T., Kusachi, S., Yamanishi, A., Kumashiro, H., Nunoyama, H., Sano, I., Nakahama, M., Murakami, T., Naito, I., Ninomiya, Y. and Tsuji, T. 1998. Localization of type IV collagen alpha chain in the myocardium of dilated and hypertrophic cardiomyopathy. *Jpn. Heart J.* **39**: 753–762. [Medline] [CrossRef]

36. Yamanishi, A., Kusachi, S., Nakahama, M., Ninomiya, Y., Watanabe, T., Kumashiro, H., Nunoyama, H., Kondo, J., Naito, I. and Tsuji, T. 1998. Sequential changes in the localization of the type IV collagen α chain in the infarct zone: immunohistochemical study of experimental myocardial infarction in the rat. *Pathol. Res. Pract.* **194**: 413–422. [Medline] [CrossRef]

37. Zamilpa, R. and Lindsey, M. L. 2010. Extracellular matrix turnover and signaling during cardiac remodeling following MI: causes and consequences. *J. Mol. Cell. Cardiol.* **48**: 558–563. [Medline] [CrossRef]

38. Zhang, L., Wang, H., Xu, J., Zhu, J. and Ding, K. 2014. Inhibition of cathepsin S induces autophagy and apoptosis in human glioblastoma cell lines through ROS-mediated PI3K/AKT/mTOR/p70S6K and JNK signaling pathways. *Toxicol. Lett.* **228**: 248–259. [Medline] [CrossRef]